Mon. Not. R. Astron. Soc. 277, 277–286 (1995)

Imaging polarimetry of proto-planetary and planetary nebulae

S.M. Scarrott and R.M.J. Scarrott
Physics Department, University of Durham, South Road, Durham DH1 3LE

Accepted 1995 June 8. Received 1995 June 5; in original form 1995 April 20

ABSTRACT

Imaging polarimetry maps are presented for a sample of bipolar proto-planetary and planetary nebulae (Frosty Leo, Roberts 22, Hen 401, MZ 3, NGC 2346, IC 4406 and J 320). Each of the highly polarized proto-planetary nebulae possesses a 'polarization disc' which has been observed more frequently in nebulae associated with star forming regions. In order to account for the observed high levels of polarization in proto-planetary nebulae we consider the effects of a thin coating of a volatile material on refractory grains with an original size distribution typical of the interstellar medium.

The planetary nebulae are seen in a mixture of reflected and emission light and their polarization patterns suggest that, in many instances, they are emission nebulae surrounded by an extensive envelope of reflection nebulosity.

The origin of the skew-symmetry and ansae in the isophotal maps of proto-planetary and planetary nebulae are discussed in terms of binary stars and magnetic fields.

Key words: polarization – planetary nebulae: general – reflection nebulae.

1 INTRODUCTION

The relatively rapid stellar transition along the asymptotic giant branch (AGB) towards planetary nebulae is only gradually being understood. This transition, occurring over a few thousand years, is characterized by several consecutive phases including mass loss by a slow wind, a proto-planetary nebula (PPN) stage where the system first shows a non-stellar morphology, fast photo-ionizing winds and, finally, the creation of emission-line planetary nebulae (PNs).

Many PPNs and PNs have a bipolar structure consisting of two diametrically opposed lobes of nebulosity surrounding the central evolving and exciting star: the prevalence of this structure suggests that processes leading to its formation must be built into mechanisms controlling the evolution of AGB stars. The presence of an equatorial gas/dust disc in the early stages of this evolution is usually assumed to be responsible for the asymmetric expansion in the subsequent development of PPNs and PNs. The origin of the disc has had many explanations ranging from stellar rotation, non-axisymmetric magnetic fields and fossilized discs associated with single star progenitors to various aspects of interacting binary systems – the matter is still unresolved. It seems that, whatever the precise details of the origin of the disc, bipolar systems appear to require more massive progenitor stars than other forms of PPNs and PNs (Morris 1987; Corradi & Schwartz 1995).

The various stages of AGB evolution have been studied by several means and the present authors have used the technique of imaging polarimetry to investigate the structure and nature of several PPNs and young PNs (OH 231.8+4.2 – Scarrott, Rolph & Wolstencroft 1990a; IRAS 0731−0147 – Scarrott et al. 1990b; M 2-9 – Scarrott, Scarrott & Wolstencroft 1993a). Although PPNs are usually reflection nebulae seen by scattered light which is highly polarized, several established PNs, considered to be seen by direct emission-line radiation, also show significant levels of polarization.

The polarization data presented in this paper for a sample of proto-planetary and planetary nebulae are interpreted in terms of the structure and evolutionary status of these systems. Some Frosty Leo polarization data have already been published (Scarrott & Scarrott 1994) but we also include this nebula as it seems to represent the archetypal PPN and comparisons will be frequently made between it and other PPNs and PNs.

2 OBSERVATIONAL DETAILS

All the objects discussed in this paper were observed on the 3.9-m AAT with the Durham imaging CCD polarimeter (Scarrott et al. 1983; Scarrott 1991) during the period 1991 – 1993. The observations were made using a V waveband filter and a sequence of long and short exposures were made for each object in order to determine the polarization for the fainter and brighter parts of the nebulae respectively without saturating the CCD. The data were reduced in our standard manner (Draper 1988) to yield the results described in the next sections.

3 RESULTS AND DISCUSSION

Prior to describing our results it will be helpful to make a few general comments about polarization features that arise from the various geometries and grain properties found in bipolar

nebulae combined with any effects induced by extinction in the interstellar medium (ISM). Following this we will discuss the results in detail for each object before undertaking a general discussion.

3.1 A summary of known polarization features of bipolar nebulae

For a simple reflection nebula with a central illuminator the pattern of polarization vectors is expected to be centro-symmetric about the illuminating source (and this is the case even if we cannot see the illuminator directly). For systems seen by a mixture of reflected central starlight and gaseous line-emission from the extended nebulosity we still expect this pattern because the line-emission radiation will be unpolarized and only serves to dilute the polarized scattered light.

There are two main causes for deviations from a centro-symmetric pattern even in the situation of a single central illuminator. In some directions close to the galactic plane the ISM polarizes light passing through it via dichroism by magnetically aligned grains (typically $\leqslant 5$ per cent). If we view a PPN or PN in one of these directions polarization will be induced in addition to any polarization already created in the object itself. This dichroism affects the reflected and gaseous emissions equally and can produce rather complicated vector patterns as we shall see in later sections. Another cause of deviations occurs when a part of the extended nebulosity cannot see the source directly and is illuminated by light that has already been scattered at least once. The pattern produced by multiply scattered light depends on the given geometry but the ubiquitous 'polarization disc' seen in pre-main-sequence bipolar nebulae probably originates in this manner (Menard & Bastien 1988; Scarrott, Draper & Gledhill 1992; Whitney & Hartmann 1992; Scarrott & Scarrott 1994).

3.2 The proto-planetary nebulae

In this section we present data for objects which are usually classed as PPNs on the basis that their central stars are heavily or totally obscured from our direct view.

3.2.1 The Frosty Leo

This is a bipolar reflection nebula illuminated by a central star which is hidden from direct view at optical wavelengths by an obscuring circumstellar disc (Hodapp, Sellgren & Nataga 1988; Rouan et al. 1988). The material in the dusty lobes has a component of water ice (Forveille et al. 1987; Likkel et al. 1987) and a recent optical study (Scarrott & Scarrott 1994) has found very high levels of polarization ($\approx$ 60 per cent in *I*). IR observations of the inner regions of this nebula have shown that the central star is binary in nature (Roddier et al. 1995).

In Fig. 1 we present intensity contour and polarization maps of the nebula. The intensity isophotes show the bright double-lobe structure in the centre surrounded by more diffuse nebulosity with relatively bright ansae at $\approx$ 12-arcsec offset distances along the major axis of the nebula. The isophotes show a skew-symmetric symmetry culminating in the outer ansae. The polarization map shows that at offsets $\geqslant 6$ arcsec the pattern of vectors is centro-symmetric and centred on the

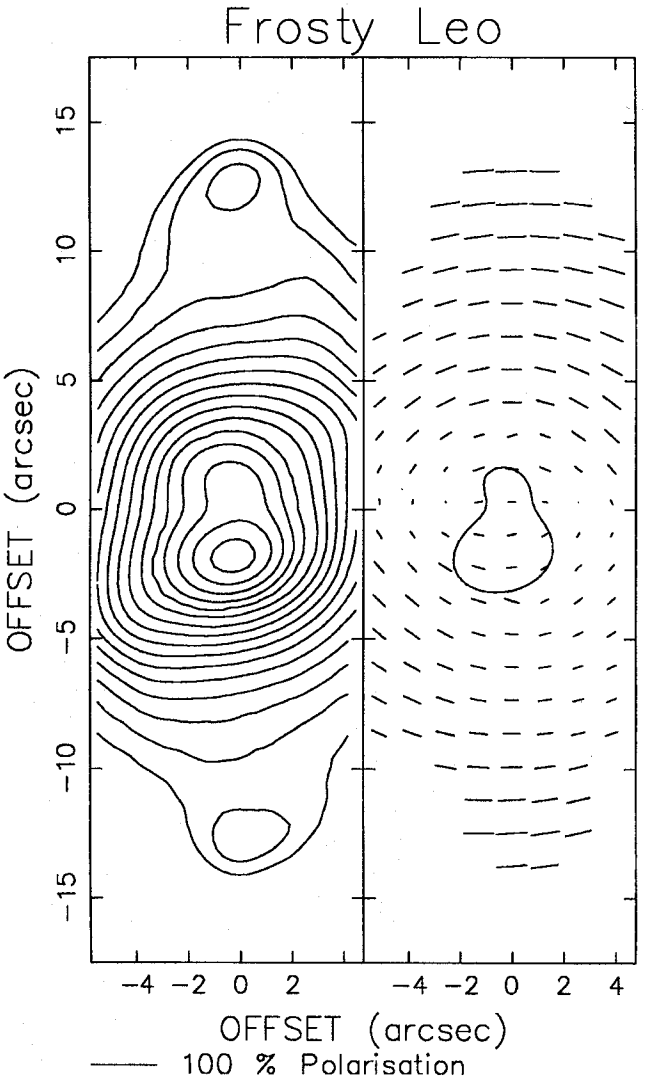

Figure 1. The Frosty Leo Nebula. Left: an intensity contour map. Note the skew-symmetry in the isophotes culminating in the ansae. Right: the polarization map superposed on an isophote representing the bright inner region. Beyond ± 6 arcsec from the centre the pattern of vectors is circular and typical of a reflection nebula illuminated by a central source which is located between the two bright lobes of nebulosity and, in this case, hidden from our direct view. The ansae at ± 12 arcsec are highly polarized (45 per cent in *V*). The non-circular pattern in the inner 6 arcsec represents the 'polarization disc'.

dust lane which appears to bisect the two bright inner lobes. There is no star-like optical feature at the location of the illuminating source (i.e. at the centre of the vector pattern) which confirms that the source is hidden from direct view by circumstellar material. The pattern of vectors in the inner 6 arcsec has the form of a swathe of polarization vectors with null points (zero polarization) at $\approx$ 3-arcsec offsets in the equatorial plane of the nebula. This inner pattern appears to be similar to the 'polarization disc' seen in many pre-main-sequence objects where it is widely attributed to the effects of a circumstellar disc. The skew-symmetry and/or polarization disc geometry have been seen before in the Frosty Leo (Morris & Reipurth 1990; Scarrott & Scarrott 1994) and

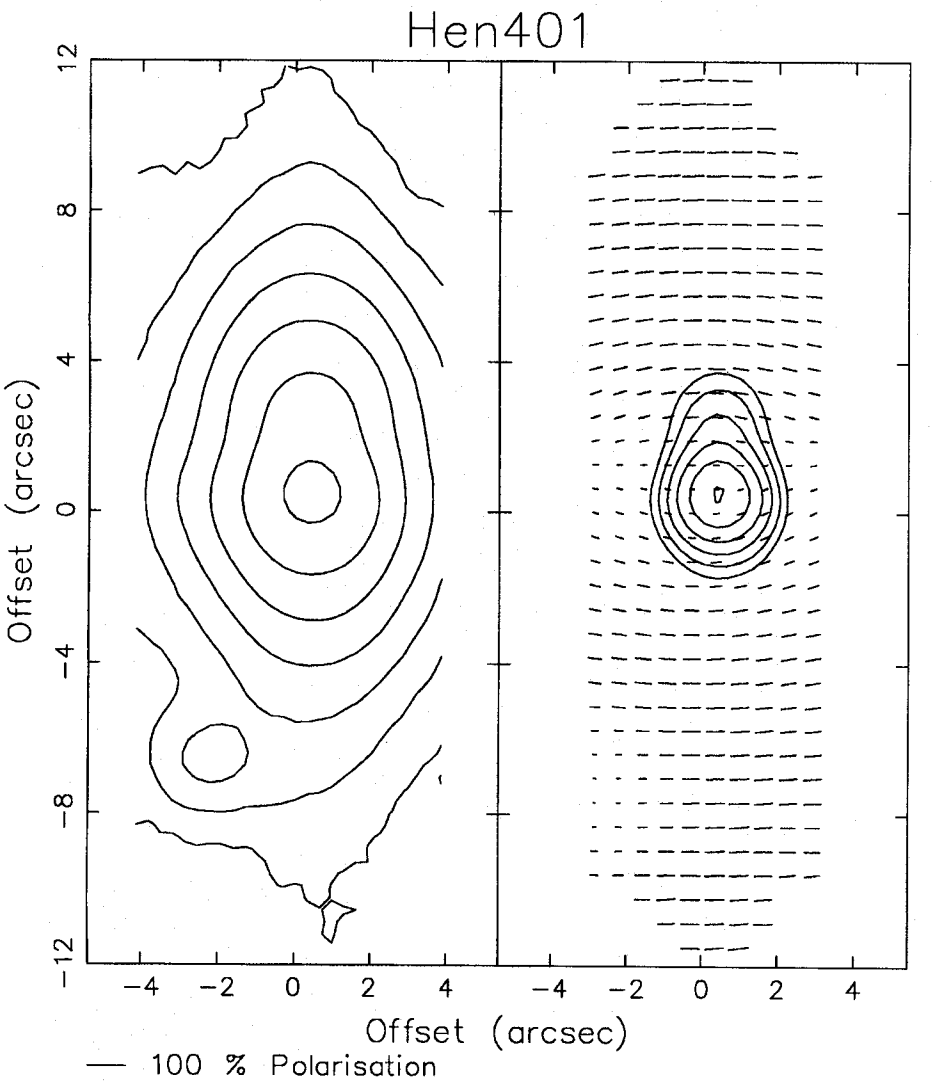

Figure 2. The Hen 401 Nebula. Left: an intensity contour map. Note the vestigial ansae on the major axis at ±12-arcsec offset. Right: the polarization map superposed on the brighter isophotes. Note the similarities with the Frosty Leo and Roberts 22.

other PPNs (e.g. OH 231.8+4.2 – Scarrott et al. 1990a; Kastner & Weintraub 1995).

3.2.2 *Hen 401*

Hen 401 is a small nebula whose central star is embedded in bright nebulosity and not clearly resolved from it. On the basis of an optical spectrum of the nebulosity Bujarrabal & Bachiller (1991) classify the central star as B1 with $\approx 3-4$ mag of extinction, presumably circumstellar in origin.

Our results are shown in Fig. 2. The intensity contour map shows a small elongated central nebula with a slight waist in the inner isophotes ≈ 2 arcsec N of the central brightness peak. This brightness structure, the circular polarization pattern and the presence of the 'polarization disc' are all consistent with Hen 401 being a bipolar reflection nebula with a central illuminating star which is totally obscured from our direct view by a circumstellar disc. We note also that there are small narrow projections in the brightness distribution some 10 arcsec to the N and S of the central brightness peak; these are reminiscent of, but not identical to, the ansae seen in the Frosty Leo.

3.2.3 *Roberts 22*

Roberts 22 is a small bipolar reflection nebula with a hidden illuminating star of spectral type A2Ie (Allen, Hyland & Caswell 1980). It is also an OH maser (OH 284.18–0.79 – Manchester, Goss & Robinson 1969) and a strong IR source (IRAS 10197–5790), and shows CO emission (Bujarrabal & Bachiller 1991).

Our polarization results are shown in Fig. 3. The optical morphology, including the 'polarization disc', is very similar to that of the Frosty Leo Nebula and Hen 401 except that the ansae are absent.

3.3 The planetary nebulae

In this section we present data for objects which are usually considered to be PNs on the basis that they are seen mainly

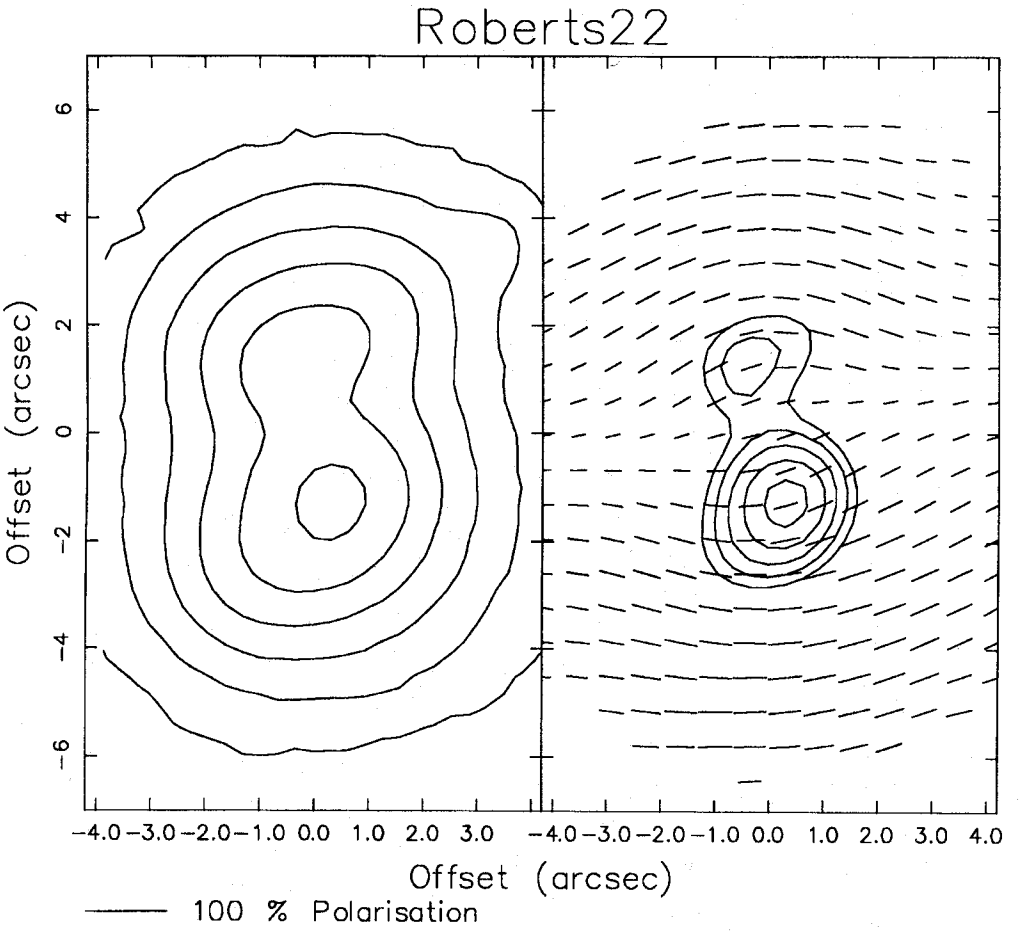

Figure 3. The Roberts 22 Nebula. Left: an intensity contour map. Right: the polarization map superposed on the brighter isophotes. Note the similarities with the Frosty Leo and Hen 401.

by emission-line radiation from an extended and hot gaseous medium.

3.3.1 MZ 3

This nebula has bright inner lobes, seen mainly by emission-line radiation, and fainter and more amorphous outer ones. Velocity measurements show expansion in the inner lobes and that the system is tilted with respect to our line of sight with the southern lobe directed towards us (Lopez & Meaburn 1983; Meaburn & Walsh 1985).

Our results are illustrated in Fig. 4. The central frame shows an intensity contour map in which the bright inner lobes are quite conspicuous. The narrow waist ≈ 2 arcsec N of the bright central core is presumably due to the obscuration induced by the circumstellar disc, and the effects of this, and the proposed tilt of the system to our line of sight, lead to the differences in the appearance of the two bright lobes. The left hand frame shows a polarization map which does not show the simple and large-scale centro-symmetric pattern of vectors as might be expected. Certain areas, notably at offsets $\geqslant 15$ arcsec to the S and to the NW, show the expected pattern but in the inner brighter regions the nebulosity seems to be polarized at position angles of $\approx 60° - 90°$. The central core is also polarized (4.5 per cent at 74°) in a similar manner to the bright (emission-line-dominated) nebulosity which suggests that there is a component of polarization induced by the ISM. If we assume that the core is intrinsically unpolarized then we can allow for the effects of the ISM, and the right hand frame in Fig. 4 shows the corrected map. This pattern is much more centro-symmetric and is typical of a system seen in a combination of reflected and emission-line radiation.

There are areas of high and low polarization corresponding, respectively, to the reflection and emission components dominating the light reaching us. The southern lobe is quite remarkable: there is a circular area ≈ 12 arcsec in diameter centred some 6 arcsec S of the core which is almost unpolarized, yet around this there is a ring of enhanced polarization (10–20 per cent). In Fig. 5 we show intensity (left) and polarized intensity (right) images of MZ 3: the polarized intensity image emphasizes the ring-like nature of the southern lobe. The polarization data taken in conjunction with the velocity measurements indicate that the inner southern lobe is a spherical cavity – a bubble – with dust concentrated on its surface. The northern lobe is more complex but this may be due to the effects of an overlying dusty disc.

Beyond the inner bright lobes the fainter nebulosity shows significantly higher levels of polarization typical of reflection nebulosity. It appears that these regions represent an outer

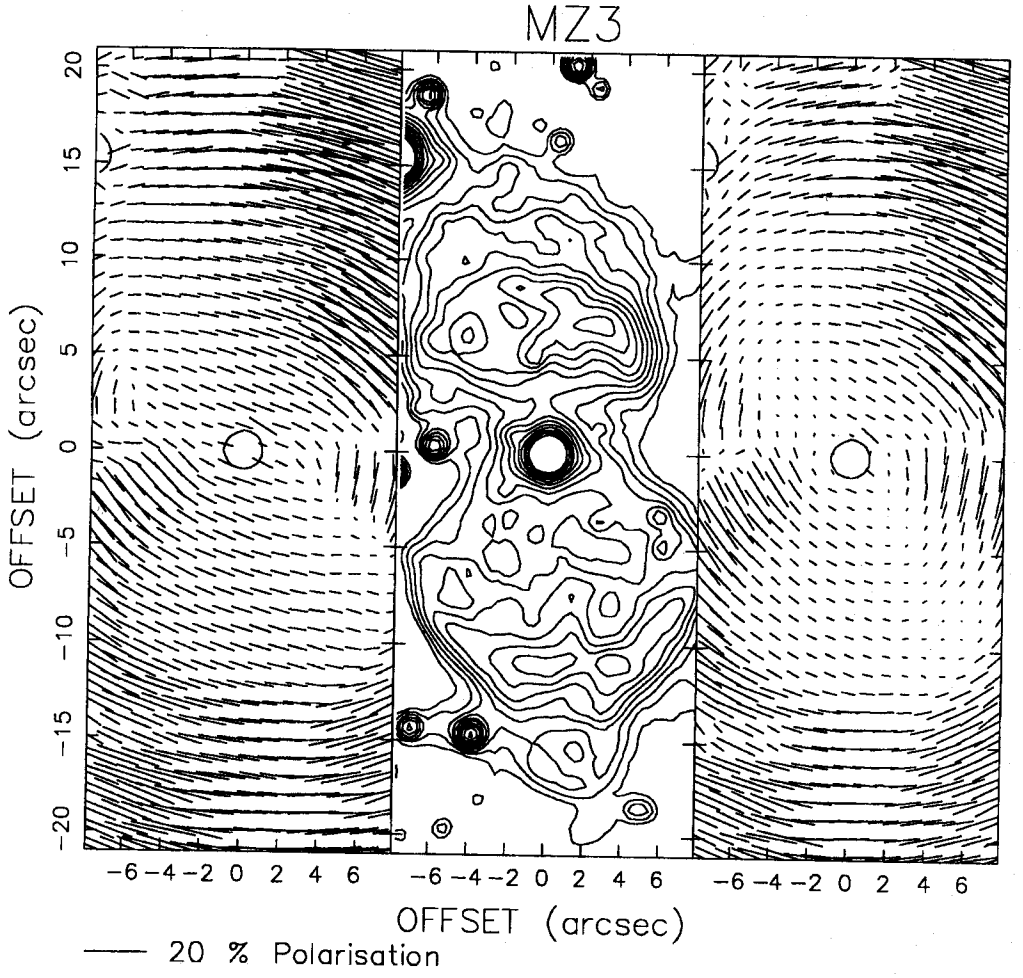

Figure 4. The MZ 3 Nebula. Left: the original polarization map uncorrected for interstellar polarization. Centre: an intensity contour map. Right: the polarization map after correction for interstellar polarization.

tenuous envelope which contains only neutral and dusty material which scatters the starlight from the bright inner regions of the system. MZ 3 has the appearance of an emission nebula surrounded by a faint and extensive reflection nebulosity.

3.3.2 NGC 2346

This nebula has a bipolar structure with open ends and is seen mainly in emission-line radiation. There is evidence for an extensive circumstellar disc and the whole system seems to be significantly tilted with respect to our line of sight so that the central core can be seen over the edge of the disc. This central core is a close spectroscopic binary with a main-sequence A star as the dominant component at optical wavelengths, but the ionizing radiation, exciting the nebula, must come from the other component (Balick 1987; Icke, Preston & Balick 1989).

Fig. 6 shows our results. The levels of polarization are low, indicating that the light reaching us is mainly emission-line radiation from the hot nebular gas rather than reflected starlight. The polarization vectors exhibit a more elliptical pattern rather than a circular one, which suggests that the illuminator is slightly elongated along the minor (E–W) axis of the nebula. The isophotes are slightly pinched to the N of the core and this represents the obscuring effects of the disc. A simple interpretation of the polarization data is that we are seeing light scattered by dust distributed along the edge of the disc against a background of unpolarized light from the ionized nebular medium. This interpretation is supported by the presence of H_2 emission that is also distributed along the edge of the disc and the walls of the bipolar lobes (Kastner et al. 1994). The pinching of the isophotes and the difference in levels of polarization between the N and S lobes confirm that we are seeing the system at a considerable angle of tilt (Icke et al. 1989 quote 40° and we have no reason to question this value).

3.3.3 IC 4406

This nebula has been imaged in various lines and mapped in shocked H_2 and CO emission (Peimbert & Torres-Peimbert 1984; Sahai et al. 1991). The optical image is bipolar and cylindrical with its major axis along an E–W direction whereas the shocked H_2 emission is concentrated at 12 arcsec to the N and S of the relatively faint and centrally located exciting star. These features along with CO velocity maps led Sahai et al. (1991) to propose a model for the system which includes elongated cavities (seen as the cylindrical nebular lobes) exca-

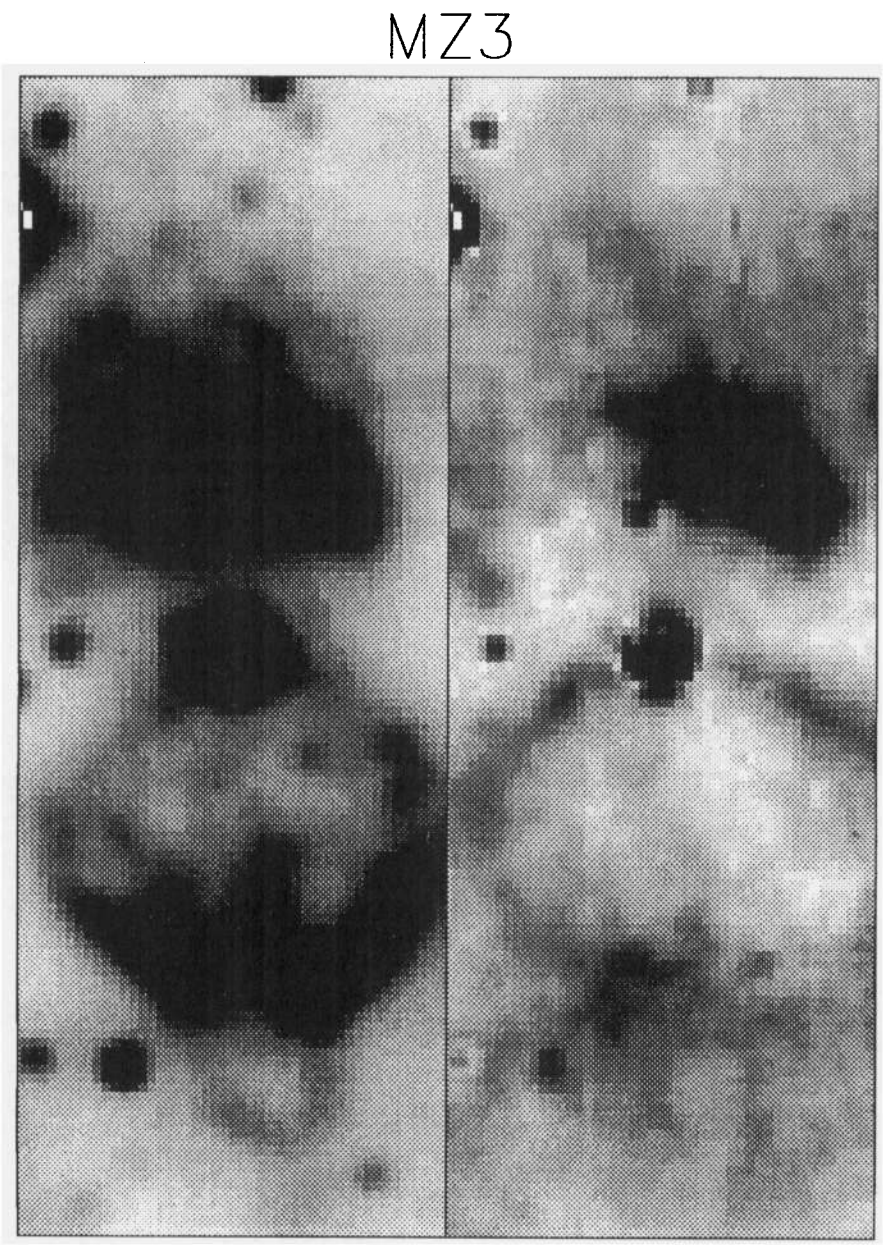

Figure 5. The MZ 3 Nebula. Left: a grey-scale intensity image. Right: a grey-scale polarized intensity image. This image shows the limb brightening around the edge of the emission-line bubble – dust has been snowploughed on to the surface of the bubble. The dimensions of each of these frames are 13 arcsec by 42 arcsec.

vated by recent high-velocity outflows into an extensive outer envelope of pre-existing neutral material.

Fig. 7 displays our polarization results. The intensity contours represent the cylindrical bipolar nebula seen by emission-line radiation. The bunching of the contour lines along the N–S direction in the central region suggests the presence of a concentration of obscuring material presumably in the form of a circumstellar disc. In the contoured region we do not detect any significant polarization which confirms that this region is seen by (unpolarized) emission from a hot gas rather than by scattered (polarized) light from the central star. However, in the fainter regions beyond the emission-line nebulosity, there are significant levels of polarization (up to $\approx$ 20 per cent) with the polarization vectors forming a centro-symmetric pattern surrounding the central star; these features are typical of a simple reflection nebula. IC 4406 is an emission-line planetary nebula embedded in extensive reflection nebulosity with the central star acting as both the illuminating source of the reflection nebula and the origin of the collimated outflows giving rise to the emission-line radiation and the H_2 and CO emission.

3.3.4 J 320

This is a very small bipolar nebula with symmetrically placed double ansae. We were unable to detect any coherent polarization pattern in this object at levels in excess of 0.25 per cent which suggests that any scattered light must be totally

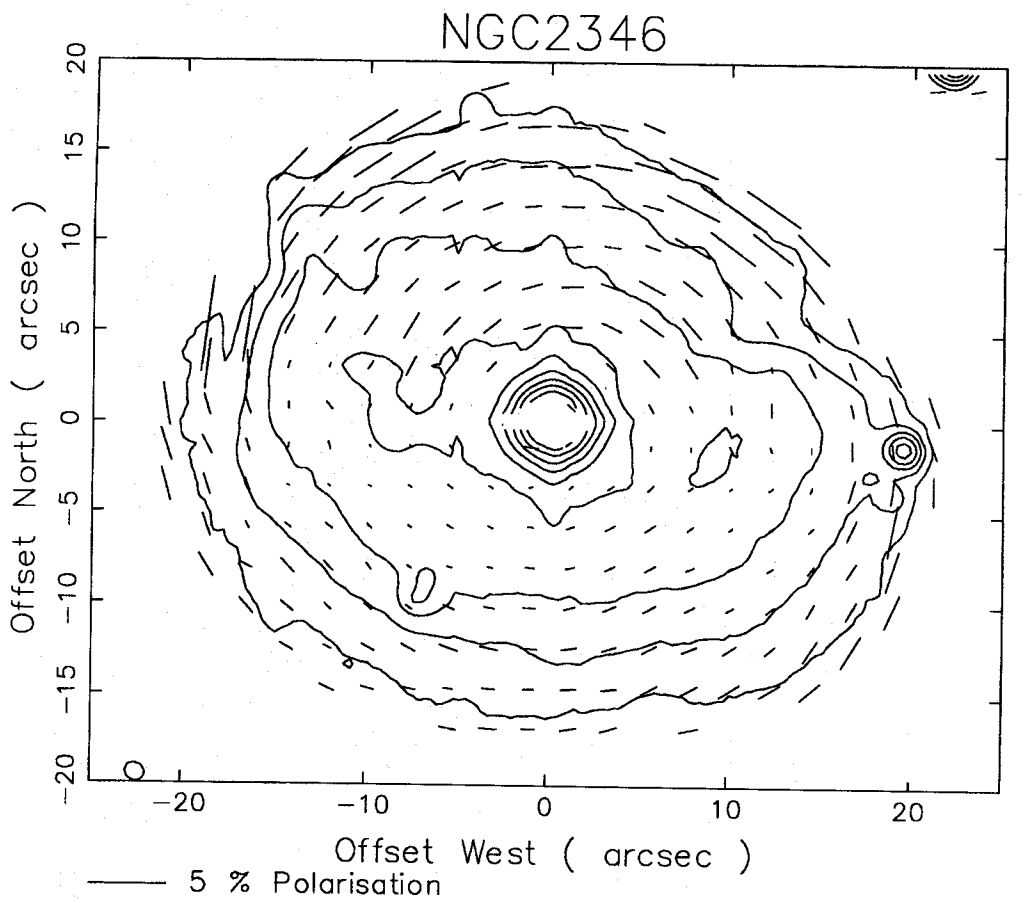

Figure 6. The NGC 2346 Nebula. This shows the polarization data superposed on an intensity contour map. The polarization to the north is significantly higher than in the south.

overwhelmed by emission radiation. However, we include this object to draw further attention to remarkable symmetries shown in the isophotes in Fig. 8. We assume that the bright spot at the origin of our coordinate system is the central star on the grounds that it is at the centre of symmetry of a rather complex set of isophotes. However, the knot 3 arcsec to the SE does give the innermost region a semblance of bipolarity with a hidden source. In the inner ± 5 arcsec the symmetry axis is around 120° but it gradually changes to $\approx 170°$ for the outermost ansae. The whole nebula shows a beautiful skew-symmetry (sometimes referred to as point reflection) akin to the one seen in the Frosty Leo PPN.

3.4 General discussion

Most of the objects displayed in this paper show polarization effects which can be linked to the features – geometry and dust properties – of the nebulae. In terms of the polarization results the objects may be divided into two distinct groups, those seen purely by reflection with high levels of polarization and referred to as PPNs, and those seen in a combination of reflection and emission-line radiation, the PNs, which have lower levels of polarization.

The PPNs (Frosty Leo, Hen 401 and Roberts 22) are all relatively young with the central stars hidden from our direct view at optical wavelengths by dense circumstellar material. If this material is in the form of a disc (or torus) then light escaping along the polar axes of the discs illuminates the outer material to create the visible reflection nebulae. In each of these objects we find evidence for a 'polarization disc' – a swathe of polarization vectors aligned parallel to the minor axis of the nebula – which is frequently seen in pre-MS bipolar reflection nebulae. In the ISM the alignment of simple paramagnetic grains takes $\approx 10^6 - 10^7$ yr (Dolginov 1990) so it is unlikely that in PPNs the 'polarization disc' is produced by dichroism by aligned grains in the disc for the simple reason that there is insufficient time for the grains to align themselves in the transient PPN stage – a more acceptable explanation lies in multiple scattering. The central disc is so opaque in its central plane that light cannot escape in this direction but does travel more freely along the polar direction and, if this light is scattered just above the central dense disc, it can illuminate the outer, more tenuous parts of the disc to be scattered again into our line of sight. In the first scattering, polarization will be induced parallel to the plane of the disc, but in the second, and subsequent scattering, another sense of polarization will be impressed on the radiation and, in certain circumstances, this can completely offset that from the first scattering – this leads to polarization null points. In each case we see the expected null points on the minor axis of the nebula on either side of the hidden illuminator.

The 'polarization disc' is not seen in the more advanced PNs simply because the central stars are no longer heavily

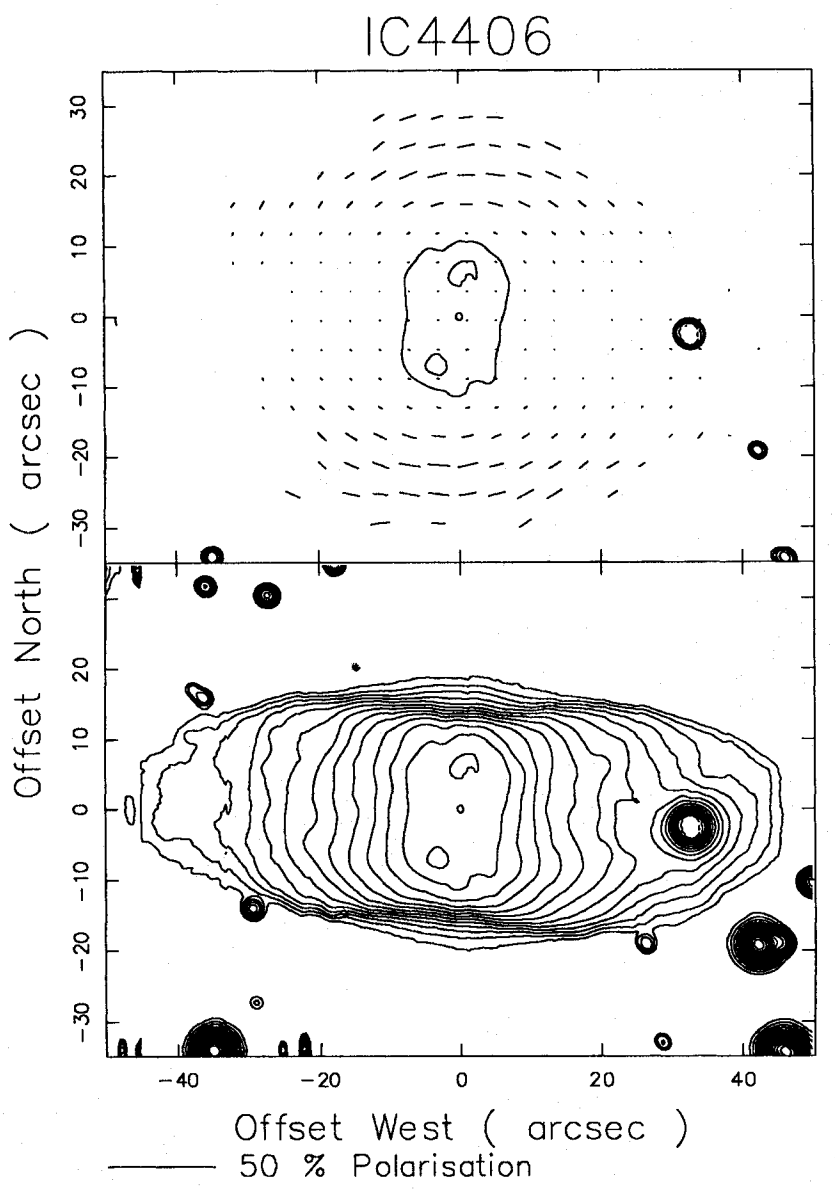

Figure 7. The IC 4406 Nebula. Top: a polarization map superposed on the brighter contours. Bottom: an intensity contour map.

obscured in the plane of the disc and can illuminate everywhere directly. We recall that the Boomerang Nebula and IRAS 0731−0147 (Taylor & Scarrott 1980; Scarrott et al. 1990b) are both highly polarized bipolar PPNs with apparently directly visible stars which would suggest that these represent the older PPNs with less obscure inner discs. Of these two objects, only the Boomerang Nebula has a 'polarization disc' which suggests that disc obscuration remains only very close to the central star. In the multiple scattering explanation of the 'polarization disc' it must be realized that the positions of the null points only represent the location in the geometry of the system where the effects of the competing scattering processes are a maximum; they do not indicate the extent of the obscuring disc which is presumably much smaller and, in the case of the Boomerang Nebula, may not be resolved from what is perceived as a central star.

The grains that are responsible for most of the optical extinction in the ISM are usually assumed to be silicates with a power-law size distribution of the form $n(a) = a^{-m}$ with the index $m = 3.5$ for the canonical prescription (Mathis, Rumpl & Nordsieck 1977, MRN). A obvious source of these grains is in the condensatory environment of the atmospheres of evolving stars, particularly red giants. If this is the case we might expect to see the nascent ISM material in the outer envelopes of the PPNs we have investigated. However, Mie scattering from a MRN mix of grains only gives rise to ≈ 30 per cent polarization under ideal conditions (optically thin scattering at angles at $\approx 90°$), yet in many of the PPNs the levels of polarization are almost double this value. Calculations of the power-law size distributions necessary to explain the PPN levels of polarization invariably require an index $m \geqslant 5.0$ which implies a preponderance of smaller grains. However, grains of sizes < 0.1 μm do not contribute as much as one might expect to scattering and extinction at optical wavelengths because their effective cross-sections are much less than their geometrical ones. As a consequence, the maximum contributions to scat-

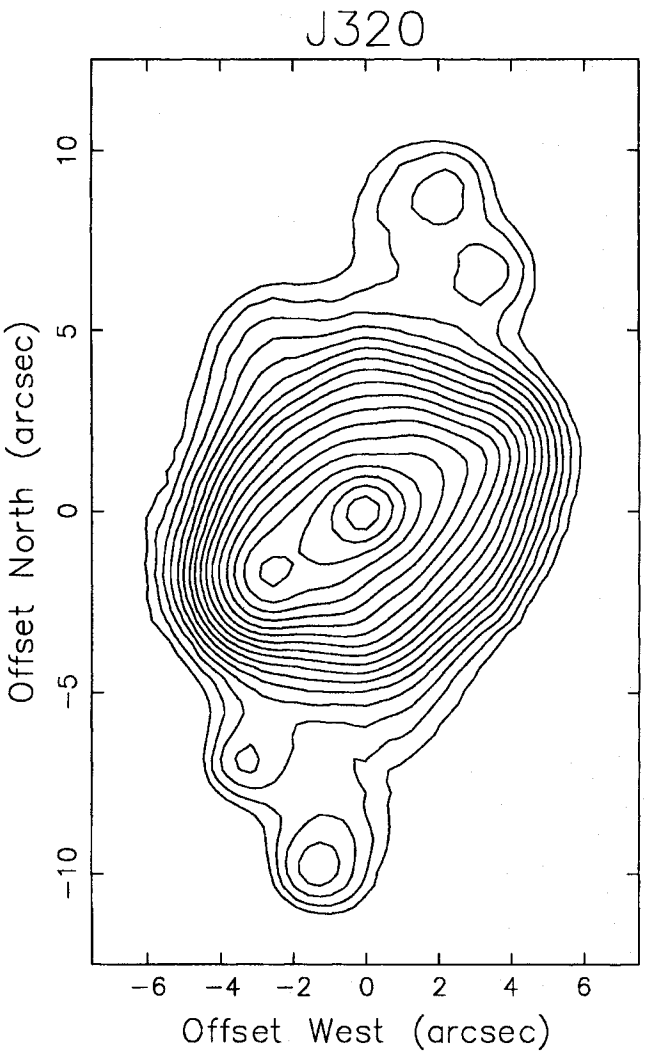

Figure 8. The J 320 Nebula. This shows an intensity contour map. The bright nebulosity is unpolarized at levels $\geqslant 0.25$ per cent. The intensity isophotes show quite remarkable skew-symmetry culminating in the outer ansae.

tering come from grains of sizes 0.1−0.2 μm since these are the most abundant grains with effective geometrical cross-sections. In the course of our earlier work on the Frosty Leo using calculations for composite silicate/ice grains, it was necessary to invoke an index of ≈ 5.5 with a lower grain size cutoff of 0.1 μm. Barlow (private communication) suggested to us that our distribution might arise if silicate grains with a typical ISM distribution are covered with a uniform thin layer (≈ 0.1 μm) of ice. Recent calculations on core mantle grains (Fullerton & Scarrott, in preparation) indicate that the addition of a uniform thin coating will explain the high polarizations in the Frosty Leo and other PPNs.

The scenario in which refractory cores with ISM properties are created in the atmospheres of evolving stars and then thinly coated (with volatiles such as ice or carbonaceous material) in the cooler outer envelopes of PPNs, giving rise to the observed polarization results, seems quite tenable, especially if one accepts that the more volatile coating is eroded or removed in the more hostile ISM environment, thus returning the dust features to their ISM characteristics. The scenario could be carried a step further to include a succession of coatings whenever grains enter the dark clouds involved in star formation, thus accounting for the high 30–50 per cent polarization seen in pre-MS bipolar nebulae (e.g. LkHα 208 – Shirt, Scarrott & Warren-Smith 1983; Parsamyan 22 – Scarrott, Draper & Tadhunter 1993b). The concept of thinly coated grains is quite important as it allows a canonical ISM mix of grains to be modified temporarily into one in which the usually ineffective yet highly abundant grains of size $\leqslant 0.1$ μm become the most prolific scatterers (and extinguishers if the albedo is high).

The PNs MZ 3 and NGC 2346 are seen in a combination of reflected and emission-line radiation so that the interpretation of the level of polarization is complicated because it involves both the scattering geometry and the relative admixture of polarized reflected and unpolarized emission light. In addition, the diluting effect of the latter component reduces the levels of polarizations to an extent such that the small contribution from ISM polarization becomes significant. Regardless of these complications, there is still much to be learnt from the pattern of polarization vectors and the distribution of polarized intensity (the product of degree of polarization and intensity at any point). A polarized intensity image isolates the reflected and the emission components throughout the nebula.

MZ 3 appears to be an inner emission nebula surrounded by a more amorphous reflection nebulosity. The emission regions, particularly the southern lobe, look very much like cavities or bubbles excavated in an extensive envelope. The bright rim in polarized intensity images suggests that material has been snowploughed on to the periphery of the cavity during the resurgent outflows into a pre-existing envelope. MZ 3 represents a prime example of the effects of the two-component wind models evoked to describe PPNs and PNs. The extensive outer envelope, the result of an earlier slow wind with its high mass loss, is seen in reflection while the bubbles are the effects of the subsequent fast wind ploughing into the envelope. The interface between the two regimes is shown very elegantly in the polarized intensity image. MZ 3 represents the transitional point between PPNs and PNs.

We see no outer reflection nebulosity in NGC 2346; this system appears to have blown its way out of any envelope (or even dissipated it fully) and the only scattered light that we see is from the edges of the extensive disc of dust. However, its appearance as far as we are concerned might be influenced by the fact that it is viewed at quite an angle of tilt. If NGC 2346 does represent a tilted bipolar PN then it seems to us that it is unlikely that a bipolar seen close to pole-on would be easily recognised and classified as such. However, Kastner et al. (1994) have argued that the Ring Nebula may be similar in structure to NGC 2436 and other H_2-emitting PNs, and may be viewed close to pole-on.

IC 4406 seems to represent the later stages of the evolution towards a PN because the bright cylindrical body of the nebula is virtually unpolarized and seen almost totally by emission-line radiation. The central star is very hot and hardly stands out against the nebula, yet acts as a source of illumination of very faint and extensive reflection nebulosity along the minor axis of the nebula. It appears that even at the later stages of evolution to PNs there are still vestiges of the earlier circumstellar disc or red giant envelope, and these remnants may be more common and longer lasting than anticipated. Imaging polarimetry is quite a sensitive technique for detecting

these faint envelopes because they betray their presence by being highly polarized. Our observations presented here were made with the intention of investigating the central brighter systems, and a deeper study may reveal that the envelopes are much more spatially extended than we have shown already.

The existence of ansae in PPNs and PNs has been known for some time and in our data we find two classic examples in nebulae (Frosty Leo and J 320) which also show beautiful skew-symmetic symmetry in their isophotes. This symmetry in PPNs and PNs is not uncommon: a cursory glance at the detailed CCD images provided by Schwartz, Corradi & Melnick (1992) suggests to us that the PPN/PN objects NGC 3918, M 1-3, He 2-141, He 2-186, NGC 6309, IC 4634, Hb 5, IC 4599, He 2-434 and NGC 7009 possess skew-symmetry, and this is not an insignificant fraction of their sample bearing in mind that this symmetry may only be detected at certain viewing aspects. These nebulae, representing the whole of the evolutionary chain between PPNs and PNs, appear to share a common structure with many pre-MS bipolar nebulae (e.g. Parsamyan 22, NGC 2261/RMon), which suggests that there is a common factor influencing the evolution of pre- and post-MS bipolar nebulae.

Non-axisymmetric magnetically braked collapse and the resulting 'bunching' in the magnetic field configuration have been invoked to account for the skew-symmetry found in pre-MS bipolar nebulae (Warren-Smith 1987; Warren-Smith, Draper & Scarrott 1987). In post-MS evolution leading to bipolar nebulae the central stars have often been considered to be binary in order to explain the bipolar outflows and, although we considered magnetic effects as a possible explanation for this symmetry in the Frosty Leo, the more recent observation that the Frosty Leo is a binary system (Roddier et al. 1995) gives more credence to the possibility that binary cores are more effective in producing this particular symmetry. However, Roddier et al. (1995) require the tidally interacting influence of a third more distant star to account for the skew-symmetry, and it is most unlikely that this situation is so common as to explain all instances of this particular symmetry at both ends of the stellar evolutionary chain. It may well be that binary stars provide the common factor that links the pre- and post-MS bipolar nebulae because they remain long-term components of the central core.

We defer from totally neglecting magnetic influences because they seem to be so much a part of star formation in which skew-symmetry is so prevalent; perhaps binary stars and magnetic fields are working in tandem and account for the symmetry which appears to persist from star formation to the later stages of stellar evolution.

ACKNOWLEDGMENTS

The use of the facilities at the AAT is acknowledged. PPARC is thanked for its continuing financial support for the Durham polarimetry group. The authors wish to thank many members of the polarimetry group for their help in taking the data at the AAT at various times.

REFERENCES

Allen D.A., Hyland A.R., Caswell J.L., 1980, MNRAS, 192, 505
Balick B., 1987, AJ, 94, 671
Bujarrabal V., Bachiller R., 1991, A&A, 242, 247
Corradi R.L.M., Schwartz H.E., 1995, A&A, 293, 871
Dolginov A.Z., 1990, in Beck R., Kronberg P.P., Wielebinski R., eds, Proc. IAU Symp. 140, Galactic and Intergalatic Magnetic Fields. Kluwer, Dordrecht, p. 242
Draper P.W., 1988, PhD thesis, Univ. Durham
Forveille T., Morris M., Omont A., Likkel L., 1987, A&A, 176, L13
Hodapp K-W., Sellgren K., Nagata T., 1988, ApJ, 326, L61
Icke V., Preston H.L., Balick B., 1989, AJ, 97, 462
Kastner J.H., Gatley I., Merrill K.M., Probst R., Weintraub R.A., 1994, ApJ, 421, 600
Kastner J.H., Weintraub R.A., 1995, AJ, 109, 1211
Likkel L., Omont A., Morris M., Forveille T., 1987, A&A, 173, L11
Lopez J.A., Meaburn J., 1983, MNRAS, 204, 203
Manchester R.N., Goss W.M., Robinson B.J., 1969, ApJ, 3, L11
Mathis J.S., Rumpl W., Nordsieck K.H., 1977, ApJ, 217, 425 (MRN)
Meaburn J., Walsh J.R., 1985, MNRAS, 215, 761
Menard F., Bastien P., 1988, ApJ, 326, 334
Morris M., 1987, PASP, 195, 1115
Morris M., Reipurth B., 1990, PASP, 102, 446
Peimbert M., Torres-Peimbert S., 1984, in Flower D.R., ed., Proc. IAU Symp. 103, Planetary Nebulae. Reidel, Dordrecht, p. 233
Roddier F., Roddier C., Graves J.E., Northcott M.J., 1995, ApJ, 433, 249
Rouan D., Omont A., Lacombe F., Forveille T., 1988, A&A, 189, L3
Sahai R., Wooten A., Schwartz H.E., Clegg R.S.E., 1991, A&A, 251, 560
Shirt J.V., Warren-Smith R.F., Scarrott S.M., 1983, MNRAS, 204, 1257
Scarrott S.M., 1991, Vistas Astron., 34, 163
Scarrott R.M.J., Scarrott S.M., 1994, MNRAS, 268, 615
Scarrott S.M., Warren-Smith R.F., Pallister W.S., Axon D.J., Bingham R.G., 1983, MNRAS, 204, 1163
Scarrott S.M., Rolph C.D., Wolstencroft R.D., 1990a, MNRAS, 243, 462
Scarrott S.M., Rolph C.D., Wolstencroft R.D., Walker H.J., Sechiguchi K., 1990b, MNRAS, 245, 484
Scarrott S.M., Draper P.W., Gledhill T.M., 1992, in Gondhalekar P.M., ed., Proc. Astronomy and Astrophysics Workshop on Dusty Discs. RAL-92-084, p. 8
Scarrott S.M., Draper P.W., Tadhunter C.N., 1993b, MNRAS, 260, 171
Scarrott R.M.J., Scarrott S.M., Wolstencroft R.D., 1993a, MNRAS, 264, 740
Schwartz H.E., Corradi R.L.M., Melnick J., 1992, A&AS, 96, 23
Taylor K.N.R., Scarrott S.M., 1980, MNRAS, 193, 321
Warren-Smith R.F., 1987, QJRAS, 28, 298
Warren-Smith R.F., Draper P.W., Scarrott S.M., 1987, MNRAS, 227, 749
Whitney B.A., Hartmann L., 1992, ApJ, 395, 529

This paper has been produced using the Royal Astronomical Society/Blackwell Science LaTeX style file.